Compensatory Grasping with the Parallel Jaw Gripper[1]

Tao Zhang, Gordon Smith, Ken Goldberg
UC Berkeley[2]
Submitted to the 4th Workshop on Algorithmic Foundations of Robotics, Dec. 1, 1999

Abstract

For many industrial parts, their natural resting pose differs from the orientation desired for assembly. We have found that it is possible in many cases to compensate for this difference using a parallel-jaw gripper with fixed orientation. The idea is to arrange contact points on each gripper jaw so that the part is reoriented as it is grasped. We analyze the mechanics of compensatory grasping based on a combination of toppling, jamming, accessibility, and form closure and describe an algorithm for the design of such grasps based on the constrained toppling graph.

1 Introduction

Industrial parts on a flat work-surface will naturally come to rest in one of several stable orientations, but it is often necessary to rotate a part into a different orientation for assembly [1]. This paper proposes an inexpensive (minimalist) method for compensating for these differences in orientation by rotating the part to a desired orientation during grasping. As illustrated in Figure 1, the part is initially in stable orientation (a); it then is rotated by the gripper to orientation in (b) for assembly onto the peg. We refer to this as a *compensatory grasp*. We achieve this using a simple parallel-jaw gripper with four tips as shown in Figure 2. First, toppling tip A and constraining tip A' make contact with the part and topple it from the initial stable orientation to the desired orientation.

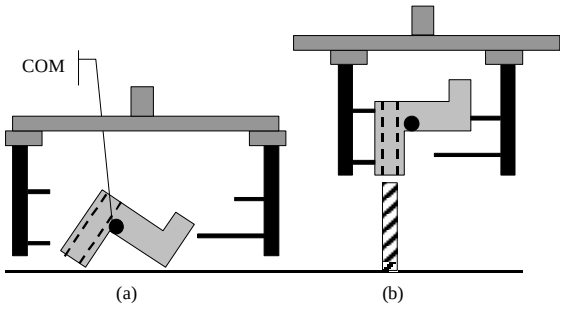

Figure 1. A compensatory grasp.

This process is referred to as "constrained toppling". Then, as soon as the part reaches the desired orientation, left fixturing tip B' and right fixturing tip B make contact, stop the part's rotation, and securely grasp it. This process is simply referred to as grasping. Note that the pivot point, C, maintains contact with bottom surface at all times.

These four tips and the parallel jaw gripper are designed to be easily reconfigurable to handle different industrial parts, and low in cost, footprint and weight.

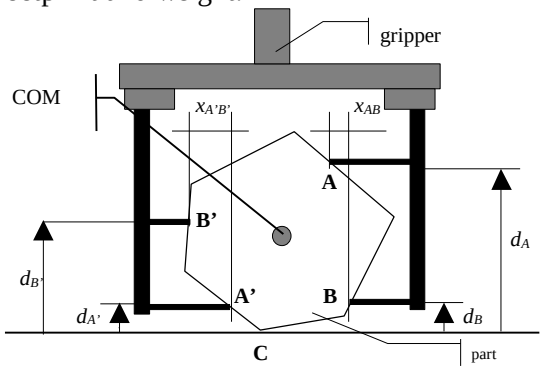

Figure 2. Terminology.

[1] This work was supported in part by the National Science Foundation under CDA-9726389 and Presidential Faculty Fellow Award IRI-9553197.
[2] Contact Goldberg@ieor.berkeley.edu, 510-643-9565.

2 Related Work

Grasping is a fundamental issue in robotics; [2] provides a useful review of research on the topic.

The two most important classes of grasps are known as *force closure* and *form closure*. The difference between these two is that the latter is stable regardless of the external wrench applied to the object. In 1990, Markenscoff *et al.* [3] proved, by infinitesimal perturbation analysis, that four hard fingers are necessary and sufficient to achieve form closure of a 2-D object in the absence of friction. The parallel jaw grippers we propose provide four contact points but the location of tips B and B' are dependent on the locations of A and A' respectively.

Mason [4] was the first to study the role of passive compliance in grasping and manipulation. Brost [5] applied Mason's Rule to analyze the mechanics of the parallel-jaw gripper for polygonal parts moving in the plane. He showed that it is possible to compensate for errors in part orientation using passive push and squeeze mechanics. Our paper considers grasp mechanics in the vertical plane.

Trinkle and Paul [6] studied grasps that lift parts while reorienting them in the vertical plane. Based upon the geometry of a grasp and quasi-static analysis, the authors generated *liftability regions*, which defines the qualitative motion of a squeezed object. They predicted the motion by solving the *forward object motion problem* that is the dual of a nonlinear program employing Peshkin's [7] minimum power principle. The pre-liftoff phase analysis of Trinkle and Paul's paper is related to our constrained toppling phase analysis in that we both applied graphic method to analyze the interaction among a planar object, a supporting surface, and a gripper in the plane containing gravity. One important difference is that we focus on the parallel-jaw gripper and consider how jaws can be designed to facilitate grasping using only translational motion.

Another approach to reorienting parts is dextrous manipulation, where the part is reoriented as it is held in force closure using constrained slip. Rus [8] proposed a *finger tracking* technique to generate rotation of grasped objects with sliding. Hong *et al.* [9] developed a planing algorithm to acquire a desired grasp by using a *finger gait* technique, which allows reposition of fingers while maintaining a grasp. Fearing [10] considered both sliding and rolling manipulation, and developed grasp planning based upon local tactile feedback, geometry, and frictional constraints. Bicchi and Sorrentino [11] analyzed the effect of rolling. Compensatory grasps combine rolling and sliding. Another approach was studied by Rao *et al.* [12]. They proposed picking up a part using a parallel gripper with a pivoting bearing, allowing the part to pivot under gravity to rotate into a new configuration.

Our work was motivated by recent research in toppling manipulation. Lynch [13] gave sufficient mechanical conditions for toppling parts on a conveyor belt in term of constraints on contact friction, location, and motion. In [14], we describe the *toppling graph* to represent the mechanics and the geometry of toppling manipulation. In this paper, we combine toppling mechanics with an analysis of jamming, accessibility and form closure.

3 Problem Definition

Given the planar projection of an n-sided convex polyhedral part **P**, how can we rotate the part to a desired orientation and grasp it securely? There are two phases involved in this process: constrained toppling and grasping. We are given as input: the part's center of mass (com), uncertainty in vertex location, ε, the coefficient of friction between the part and the surface, m_b, and the coefficient of friction between the part and the gripper, m_t. Let q denote the orientation of the part from the +X direction; initially $q = 0$. Let q_d denote the angle at the desired orientation.

During the constrained toppling phase, only gripper tips A and A' make contact with the part. We require that these two tips cause the part to rotate counter-clockwise without causing C to lose contact with the surface. From the toppling analysis in section 4 we are able to show that on a given edge, the rolling conditions are more easily satisfied if A' is lower, i.e. $d_{A'}$ is smaller. This will in general produce a finite set of possible $d_{A'}$ candidates for the part. The

height of A, d_A, can then be determined by the graphical analysis described in section 4.

The grasping phase occurs when the part has been toppled to $q = q_d$. During grasping the fixturing gripper tips, B and B', make contact with the part. We require that the contacts corresponding to A, A', B, and B' create form-closure on the part, even when friction is disregarded. Since d_A and $d_{A'}$ are already know, we must determine d_B and $d_{B'}$ such that form-closure is achieved. We additionally require that the tips B and B' do not make contact with the part before $q = q_d$. This requirement is essentially a form of accessibility constraint and further limits the possible values of d_B and $d_{B'}$. Finally, because A and B are fixed on the same jaw of the gripper (and likewise A' and B') the geometry of the part along with the relative heights of A and B will determine the relative x offset between A and B, which we denote x_{AB}.

The final output of the analysis is the height of each of the four tips, d_A, $d_{A'}$, d_B, and $d_{B'}$, as well as the relative x offset between tips on each jaw, x_{AB}, $x_{A'B'}$ (see Figure 2). This set of variables determines the gripper design that will rotate the part to the desired orientation.

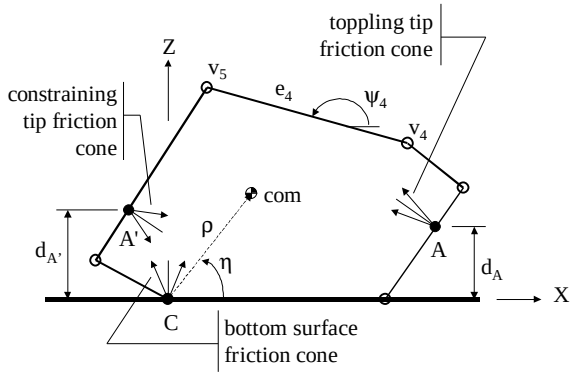

Figure 3. Notation.

Figure 3 shows the notation used in our constrained toppling analysis. The part sits on a flat worksurface in a stable orientation. The worksurface friction cone half-angle is $a_b = \tan^{-1} m_b$, and the gripper tip friction half-angle is $a_t = \tan^{-1} m_t$. The contact point between the part and the worksurface is called a pivot vertex, denoted C in figure 2, and taken to be at (0,0). The COM is a distance r from the origin and angle h from the +X direction at its initial orientation. The constraining tip, A', is a distance $d_{A'}$ from the bottom surface. We denote the vector at the left edge of the toppling tip friction cone as f_l and the right edge as f_r.

We consider **P** as shown in Figure 3. Starting from the pivot, we consider each edge of the part in counter-clockwise order, namely e_1, e_2, …, e_n. The edge e_i, with vertices v_i at (x_i, z_i) and $v_{(i+1)}$ at $(x_{(i+1)}, z_{(i+1)})$, is in direction y_i from the +X axis.

We assume that the part and the gripper are rigid, and also that the part's geometry, the location of the COM, and the position of the jaws are known exactly. We also assume that the constraining tip and the toppling tip of the gripper contact the part simultaneously, and the motion of the part and is slow enough that we can ignore inertial effects.

4 Constrained Toppling Analysis

We first consider the constrained toppling of the part. We divide constrained toppling into a rolling phase and a settling phase. Our analysis involves the graphical construction of a set of functions that represent the mechanics of these phases. In [14], we introduced the "constrained toppling graph", which includes the radius function, vertex height functions, constrained rolling height functions, and constrained jamming height functions.

The radius function, $R(q)$, is the height of the COM above the surface as the part is rotated through $q = 0 \sim 2p$. The local minima of the radius function indicate the stable orientations of the part [15], while the local maxima are unstable equilibrium orientations. In this paper we will consider only the range of angles corresponding to rotation from one single stable orientation to the next. We assume that the part can be toppled into that orientation before grasping. This range consists of the angles $q = 0$® q_n where q_n is the angle of the ext stable orientation. Additionally, q_t represents the unstable equilibrium angle in that range.

The vertex height function, V_i, gives the height of vertex i above the surface as the part rotates. Each vertex of the part has a vertex height function. We truncate V_i in two functions,

V_{ir} and V_{il}, representing the height of vertex i viewed from the +X and -X directions respectively. Using the vertex height functions we can determine which edge a gripper tip is in contact with for any q and height.

The constrained rolling height function, $H_i(q)$, is the minimum height at q that the toppling tip, A, in contact with edge e_i must be in order to roll the part given the height of A'. $H_i(q)$ is determined on the range $q = 0$® q_t. At $q = q_t$ the part is no longer being rolled, but rather is now settling under its own weight. The constrained jamming height function, $J_i(q)$, indicates a range of d_A values that may cause jamming during the settling process. $J_i(q)$ is determined on the range $q = q_t$® q_n.

All of these functions are dependant on q and map from part orientation to distance: $\boldsymbol{S}^1 \rightarrow \hat{\mathbf{A}}^+$, where $\boldsymbol{S}^1$ is the set of planar orientations. The combination of these four functions forms the constrained toppling graph from which we can height of the toppling tip A required to guarantee toppling.

4.1 Constrained Rolling Height Function

During rolling, the part rotates about C. Friction between the part and the bottom surface must not prevent C from sliding to the right, and friction between the part and the tips must not prevent the part from slipping relative to the tips. Additionally, the system of forces on the part: the contact force at the bottom surface, the contact force at the tips, and the part's weight, must generate a positive moment on the part with respective to C.

The constrained rolling height function, $H_i(q)$, is the minimum height at q and a given d that A in contact with edge e_i must be in order to roll a part. This height is determined as a function of q based on the rolling conditions derived using a graphical method from Mason [16].

As the part rolls, A' could switch edges if a contact edge is not long enough. In this paper, we consider the situation that A' keeps contact with e_i during the entire rolling phase, and the same methodology can be applied for the case where the contact switches edges (see [17] for details).

Under the assumption that A' keeps contact with e_n, relative motion direction between the part and A' is uncertain, and it depends on an angle, $(w+q)$, where w denotes the interior angle of a part at C as shown in Figure 4. We study the constrained rolling conditions based upon different $(w+q)$ ranges.

Let w_i be the distance along edge e_i as shown in Figure 4. Any point on e_i can be expressed as $(x_i + w_i \cos\gamma_i, z_i + w_i \sin\gamma_i)$.

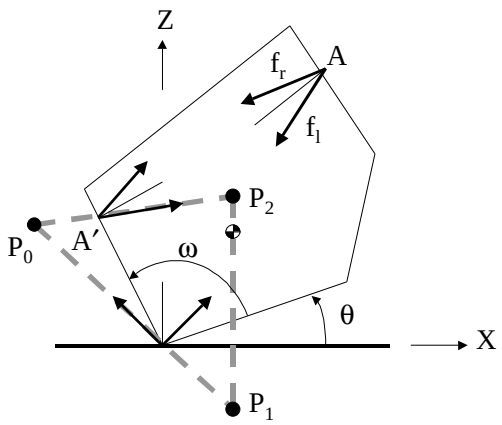

Figure 4. Rolling Conditions ($\pi > w+q > \pi/2$).

Consider the case where $\pi > w+q > \pi/2$. In such a case, rotation causes the contact between the part and A' to move away from C. To determine the constrained rolling height function, we begin by constructing a triangle as shown in Figure 4 with vertices P_0, P_1, and P_2. P_0 is determined by the intersection of the left edge of the bottom friction cone and the left edge of the constraining tip friction cone, and is at (x_{p0}, z_{p0}). P_1 is the intersection of the vertical line through the com and the left edge of the bottom friction cone, and is located at (x_{p1}, z_{p1}). P_2 is the intersection of the vertical line through the com and the left edge of the constrained tip friction cone, and is located at (x_{p2}, z_{p2}). From these definitions we have:

$$x_{p0} = g - \overline{P_0P_1}\ sin\alpha_b, \tag{1}$$

$$z_{p0} = -\ g/m_b + \overline{P_0P_1}\ cos\alpha_b, \tag{2}$$

$$x_{p1} = g, \tag{3}$$

$$z_{p1} = -\ g/m_b, \tag{4}$$

$$x_{p2} = g, \tag{5}$$

$$z_{p2} = (d/\tan(q + w) - g) / \tan(w + q + a_t), \quad (6)$$

where $$g = r \cos(h + q), \quad (7)$$

$$\overline{P_0P_1} = (z_{p2} + r \cos(q + h)/m_b) \sin(w + q + a_t)/ \sin(w + q + a_t - a_b). \quad (8)$$

Consider a region of the X-Z plane defined by linear edges. Let a *primary region* denote a region such that toppling is guaranteed if every force in the toppling tip friction cone makes a positive moment about every point in the primary region. Therefore, the $P_0P_1P_2$ triangle is the primary region in this case.

For all forces in the toppling tip friction cone to generate a positive moment about the triangle, the left edge of the friction cone must pass above the triangle; all other vectors in the friction cone will pass higher. We find the height sufficient to roll the edge by projecting lines from P_0, P_1, and P_2 at the angle of the left edge of the pin friction cone, f_l, until they intersect the edge of the part. The intersection with the maximum height of those three is the minimum height sufficient to roll the part. Notice that such a height also guarantees that C keeps touch with the bottom surface.

Let ${}_2w_i$ denote the edge contact on e_i where f_l passes exactly through point P_2. We can show through geometric construction that

$${}_2w_i(q) = (x_i \sin q + z_i \cos q - z_{p2} - (x_i \cos q - z_i \sin q - x_{p2}) \tan(b_{il} + q)) / (\cos(q + y_i) \tan(b_{il} + q) - \sin(q + y_i)), \quad (9)$$

where $b_{il} = y_i + p/2 + a_t$.

Similarly, the edge contacts for f_l passing through P_0 and P_1 are given by ${}_0w_i(q)$ and ${}_1w_i(q)$.

The constrained rolling height function, $H_i(q)$, is based on w_i which is the maximum of ${}_0w_i$, ${}_2w_i$, and ${}_3w_i$ in the rolling region $0 < q < q_t$. w_i can be shown to be

$$w_i = \begin{cases} {}_2w_i & 0 < q < q_{01} \text{ and } y_i < w \\ {}_0w_i & 0 < q < q_{01} \text{ and } y_i \geq w \\ {}_1w_i & q_{01} < q < q_m \end{cases}, \quad (10)$$

where $$q_{01} = p + a_b - a_t - y_i, \quad (11)$$

$$q_m = \min(p - y_i, p - w, q_t). \quad (12)$$

Thus, the constrained rolling height function within $0 < q < q_m$ is given by

$$H_i(q) = \begin{cases} H_i^*(q) & V_i(q) \leq H_i^*(q) \\ f & V_i(q) > H_i^*(q) \end{cases} \quad (13)$$

where $H_i^*(q) = x_i \sin q + z_i \cos q + w_i \sin(y_i + q)$. (14)

Following the same methodology, we find $H_i(q)$ under the condition $w + q = \pi/2$ and $\pi/2 > w + q > 0$ (see [17] for details).

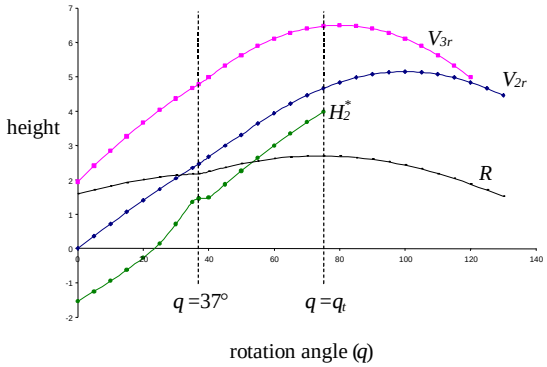

Figure 5. $R(q)$ vs. $H_2^*(q)$, $V_{2r}(q)$ and $V_{3r}(q)$.

Figure 5 illustrates the functions $R(q)$, $H_2(q)$, $V_{2r}(q)$ and $V_{3r}(q)$ for the part in Figure 3 with $a_t = 5°$, $a_b = 10°$ and $d_A = 0.9$cm. The discontinuity point ($q = 37°$) of $R(q)$ represents the orientation where e_6 is on the bottom surface. Notice that $H_2(q)$, $V_{2r}(q)$ and $V_{3r}(q)$ are also discontinuous at $q = 37°$. When $q < 37°$, V_1 is C and $x_2 = 4.1$, $z_2 = 0$, $y_2 = 56°$, $h = 46°$, $r = 2.2$, and $w = 143° - (180° - 90°) = 53°$; When $q > 37°$, V_6 is C and $x_2 = 4.6$, $z_2 = 2.4$, $y_2 = 92°$, $h = 55°$, $r = 2.7$, and $w = 89°$. At angle q any toppling tip at a height, h, such that $\max(H_2(q), V_2(q)) < h < V_{3r}(q)$ will instantaneously rotate the part. The graph indicates that A can roll the part at any contact on e_2 when $0 < q < q_t$.

Given a certain contact edge, a lower A' results in a smaller primary region; thus, a lower A will be able to topple the part. Therefore, the best location of A' on a contact edge is e above the lower vertex, i.e. A' is as low as possible. This reduces $d_{A'}$ candidates to a finite set for the

part. For each $d_{A'}$, we may employ the graphical analysis to find the feasible d_A.

4.2 Constrained Jamming Height Function

We allow the part continue to rotate after it has reached q_t if $q_d > q_t$. We call this process settling, and intend to determinate whether jamming may occur in this process. The part may jam while settling due to the frictional contact at the toppling tip. We will be conservative and eliminate any toppling tip height where jamming may occur even though we cannot be certain it will jam without further information. Note that we consider the statics (not full dynamics) of the settling process.

We only consider the situation where A' keeps contact with e_i during the entire settling phase. More general cases can be derived from the same methodology.

To determine the constrained jamming height function we begin by constructing a primary region as shown in Figure 6. Notice that there is no jamming if the constrained tip contact is left of the part gravity line, i.e.,

$$d\ tan(q+w) < r\ \cos(h+q). \tag{15}$$

Otherwise, the primary region quadrilateral with vertices P_0, P_1, P_2 and P_3. P_0 is the intersection of the vertical line through the part's com and the right edge of the constrained tip friction cone, and is located at (x_{p0}, z_{p0}). P_1 is the constrained tip contact at (x_{p1}, z_{p1}). P_2 is the intersection of the left edge of the constrained friction cone and the left edge of the bottom friction cone, located at (x_{p2}, z_{p2}). And P_3 is the intersection of the vertical line through the part's com and the left edge of the bottom friction cone, located at (x_{p3}, z_{p3}).

$$x_{p0} = g, \tag{16}$$

$$z_{p0} = d - (d\ \tan(q+w) - g)/\tan(a_t - q - w), \tag{17}$$

$$x_{p1} = d\ tan(q+w) \tag{18}$$

$$z_{p1} = d, \tag{19}$$

$$x_{p2} = -d\ \cos a_t \sin a_b / (\sin(q+w)\sin(q+w+a_t-a_b)), \tag{20}$$

$$z_{p2} = d\ \cos a_t\ \cos a_b / (\sin(q+w)\sin(q+w+a_t-a_b)), \tag{21}$$

$$x_{p3} = g, \tag{22}$$

$$z_{p3} = -\ g/m_b. \tag{23}$$

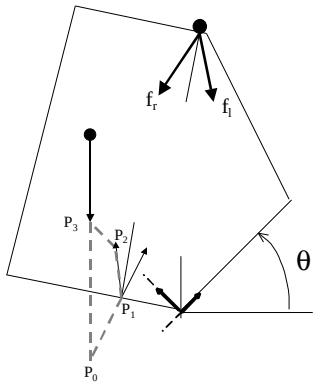

Figure 6. Jamming Conditions

To guarantee that no jamming occurs, any force in the toppling tip friction cone must make a positive moment about the critical primary region then the left edge of the friction cone must make a positive moment. In other words, the left edge of the toppling tip friction cone determines the height at which jamming may occur.

Similar to the analysis of the toppling height function, we have ${}_2w_i(q)$, ${}_0w_i(q)$, ${}_1w_i(q)$, and w_i, which is min $({}_2w_i, {}_0w_i, {}_1w_i)$ at a given q. These functions are given by:

$$w_i = \begin{cases} {}_0w_i & y_i < w - 2a_t \text{ and } q < q_{32} \\ {}_1w_i & w - 2a_t \le y_i \le w \text{ and } q < q_{32} \\ {}_2w_i & w < y_i \text{ and } q < q_{32} \\ {}_3w_i & q_{32} \le q \le p - w_k \end{cases} \tag{24}$$

where $$q_{32} = p - a_t - y_i \tag{25}$$

The constrained jamming height function, $J_i(q)$, with $q_t < q < q_n$ is given by

$$J_i(q) = \begin{cases} J_i^*(q) & V_i(q) \le J_i^*(q) \\ f & V_i(q) > J_i^*(q) \end{cases} \tag{26}$$

where $J_i^*(q) = x_i \sin q + z_i \cos q + w_i \sin(y_i + q)$. (27)

Therefore, for given q and $d_{A'}$, jamming occurs if the heights of A is lower than $J_i(q)$.

4.3 The Constrained Toppling Graph

Figure 7 illustrates the entire constrained toppling graph that combines the vertex height, constrained rolling height, and constrained jamming height functions to represent the full mechanics of toppling. From the constrained toppling graph the necessary toppling height for A can be determined or shown to be non-existent. Note that $H_i(q)$ must be bounded by the $V_{ir}(q)$ and $V_{i+1,r}(q)$ and is truncated where it intersects them.

For toppling from an initial orientation to the desired orientation to be successful, there must exist a horizontal line from the angle of the initial orientation to the angle of the desired orientation at height h that has the following characteristics:

1: $h > H_i(q)$ for all q; if $V_{ir}(q) < h < V_{i+1,r}(q)$;
2: $h > J_i(q)$ for all q; if $V_{ir}(q) < h < V_{i+1,r}(q)$;
3: $h < max(V_i(q))$ for all i at any $q < q_t$.

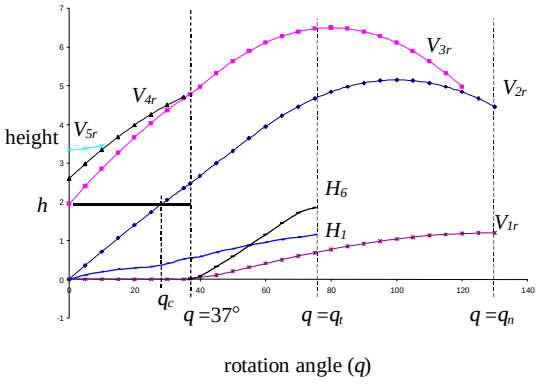

Figure 7. Constrained Toppling Graph

The first two criteria can be described as A must be above both the rolling height and the jamming height on the edge it is in contact with for all q. Note that when the pin crosses a vertex height function it contacts a new edge and must then be above the rolling height and jamming height functions for that edge. The third criterion is that the pin must not lose contact with the part by passing over it during the rolling phase.

Figure 7 demonstrates the constrained toppling graph of the part shown in Figure 3. From the graph we can determine a toppling tip at $d_{A'}$ = 2cm is capable to topple the part to any orientation with $0 < q < q_n$. Notice that A switches contact edge from e_2 to e_1 at q_c.

5. Grasping

Once the part has been rotated to $q = q_d$, the fixturing tips, B and B', must make contact with the part. Additionally, we require that the combination of the contacts corresponding to A, A', B, and B' generate a form-closure grasp on the part. There also exists an accessibility constraint on the locations of B and B' due to the requirement that they not make contact with the part until $q = q_d$. Therefor, we divide the grasping analysis into two sections corresponding to determining the accessibility constraint and meeting the form-closure requirement.

5.1 Accessibility

The accessibility constraint will limit the possible heights of the fixturing tip, B or B', for a given height of A or A'. In order to determine the accessibility constraint we must consider the relative motion between the part and a jaw of the gripper. The rest of the accessibility discussion will be in a frame of reference fixed to the toppling tip A and will consider a contact B on edge e_j. The accessibility constraint requires that as the part rotates to the desired final orientation, that it is moving out towards the fixturing tip and that at no previous angle has the part been as far out as the fixture tip and made contact.

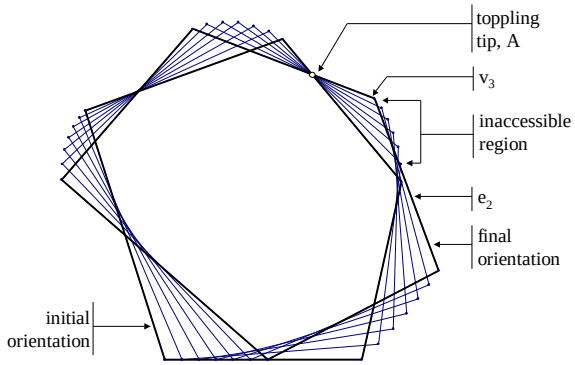

Figure 8. Rotation of a part relative to the toppling tip A.

To illustrate this situation, Figure 8 shows the rotation of a part with respect to the toppling

tip. Note that at any height within the inaccessible range on edge e_2 indicated in the figure, the location of vertex v_2 would have contacted the fixturing tip before the part reached the desired orientation. Since this would prevent the part from reaching the desired final orientation, these heights are considered inaccessible.

By examining the inaccessible region more closely, as shown in Figure 9, we can see that there are two factors to be considered when determining the accessibility of an edge. The first factor is whether any portion of the edge in the final orientation is blocked from visibility in the positive X direction by the part as it rotates. The second factor is what portion of the edge is moving forward, in the +X direction, at the final orientation.

The first factor is taken into account by calculating a vertex function for the vertex at the top of edge e_j. The vertex function gives the location of the vertex with respect to the toppling tip as a function of rotation angle. The vertex function is given by

$$x = x_j - x_i - \frac{d_A - y_i}{\tan y_i}, \qquad (28)$$

and

$$y = y_j, \qquad (29)$$

where (x_j,y_j) is the location of the vertex in the fixed frame of reference, (x_i,y_i) is the location of the vertex at the bottom of the edge that the toppling tip contacts, and y_i is the angle of that edge. We must check what portion of the edge is visible from the +X direction without being blocked by the combination of the vertex function and the initial orientation of the edge. Note that it is possible that lower edges and vertices may also block part of the final orientation of the edge, and must be checked as well. This check insures that the contact point is not blocked by the part during rotation.

The second consideration insures that the edge is moving out to the fixturing tip at $q = q_d$. In other words, the relative X displacement between A and B, denoted $\underline{x_{AB}}$, must be greater than the X location (with respect to the toppling tip) of the part at d_B for any $q < q_d$. We will denote the location of the part at a height d_B and angle q as (x_c,d_B). Note that this is a different physical point at each q.

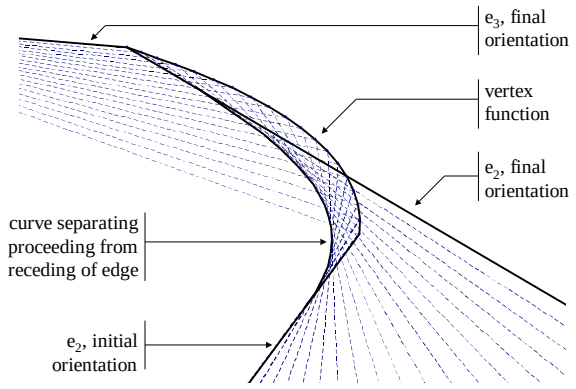

Figure 9. A portion of the edge in the final orientation may be blocked in the positive x direction before the part reaches the final orientation. Additionally, a curve shows the separation between where the part is moving forward and where it is receding.

At some critical height, h_c, the derivative of x_c with respect to q is 0. All of the physical points on that edge below h_c will meet the requirement of moving out to the part while those above will be receding. The accessibility constraint for this consideration is therefore, $d_B \leq h_c$ on a given edge.

The relative X displacement of a point of the part at height d_B can be shown geometrically to be

$$x_c = x_j - x_i + \frac{d_B - y_j}{\tan y_j} - \frac{d_A - y_i}{\tan y_i}, \qquad (30)$$

where (x_i,y_i) and (x_j,y_j) are the locations of the vertex at the bottom of the edge in contact with A and the edge in contact with B respectively, and y_i and y_j are the angles of those edges. Therefore the derivative of x_c with respect to q is given by

$$\frac{dx_{ab}}{dq} = y_i - \frac{d_A - x_i}{\tan y_i} + \frac{d_A - y_i}{\sin^2 y_i} - y_j + \frac{h_c - x_j}{\tan y_j} - \frac{h_c - y_j}{\sin^2 y_j}, \qquad (31)$$

and must be 0 at h_c. Setting (31) equal to 0 and solving for h_c yields

$$h_c = \frac{\left[y_i - \frac{d_A - x_i}{\tan y_i} + \frac{d_A - y_i}{\sin^2 y_j} - y_j \right]}{\left[\frac{1}{\tan y_j} - \frac{1}{\sin^2 y_j} \right]} \quad (32)$$

For a given edge, indicated by x_j, y_j, and y_j, only heights less than h_c can be considered when determining the height for B in the form closure analysis. A corresponding procedure is used to determine a range of possible $d_{B'}$ for a given $d_{A'}$.

5.2 Form-Closure

At the end of the accessibility considerations we now know d_A and $d_{A'}$, as well as ranges of possible values for d_B and $d_{B'}$. From these ranges we must determine values such that the four tips generate form-closure on the part. This is easily done using the method described in van der Strappen [18]. This method would entail determining the point at which the edge normals through A and A' meet, then selecting the locations of B and B' such that the edge normals through B and B' create opposite moments about that point. We omit the precise details for lack of space.

6. Experiment

We conducted a physical experiment using an AdeptOne industrial robot and a parallel jaw gripper with tips designed using the methodology described in this paper. The part is a small lever from a standard videotape (FUJI serial number: 7410161160). Its planar projection is shown in Figure 1, and its planar convex hull is shown in Figure 3.

As illustrated in Figure 1, the part begins at stable orientation (a). Its desired orientation is (b) where q =37°. We choose A and A' at d_A = 0.9 cm and $d_{A'}$ = 2.0 cm, respectively. The corresponding friction cone half angles are a_t = 5° and a_b = 10°. When q < 37°, C is V_1 and x_2=4.1, z_2=0, y_2=56°, h=46°, r=2.2, and w=143°-(180°-90°)=53°; When q > 37°, C is V_6 and x_2=4.6, z_2=2.4, y_2=92°, h=55°, r=2.7, and w =89°. The analysis yields the following tip values: d_B = 2.7 cm, $d_{B'}$ = 3.0 cm, x_{AB} = 0.0 cm, and $x_{A'B'}$ = 2.1 cm. Figure 10 illustrates the compensatory grasp.

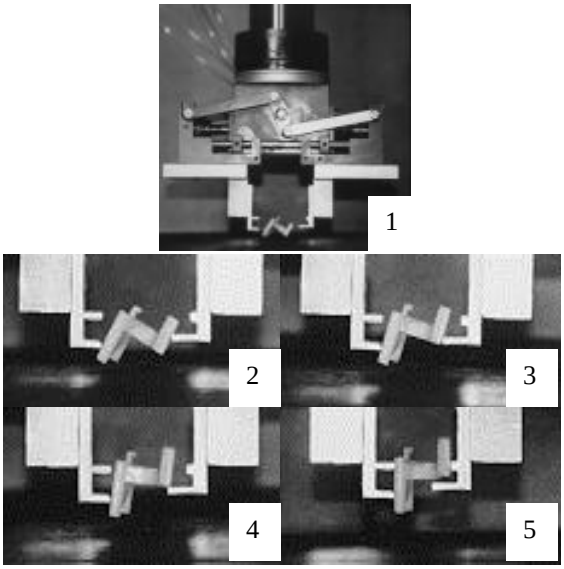

Figure 10. Compensatory grasp experiment.

7. Discussion and Future Work

In industrial practice, gripper jaw geometry is often custom-designed and machined for each part. Design has been ad-hoc and particularly challenging when the part's natural resting pose differs from the desired grip/insertion pose. In this paper we describe compensatory grasps, a new approach to this problem where 4 contact points on the jaws guide the part into alignment and hold it stably. The next step is to develop more sophisticated jaw shapes based on part trajectory (see Figure 11) and to address shape and position uncertainty, friction, and ultimately, 3D geometry. We are also interested in more efficient algorithms and knowing under what conditions a compensatory grasp exists.

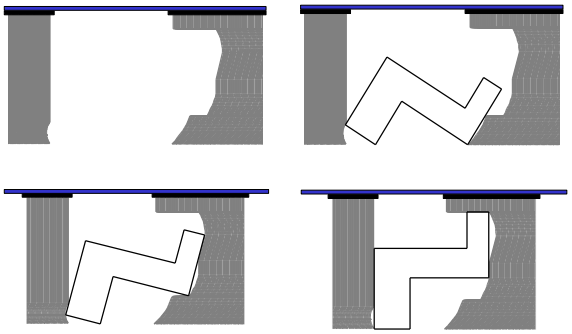

Figure 11. Gripper Jaws based on Compensatory Grasp Tips and complement of swept volume.

Acknowledgements

This paper grew out of some practical experiments with a commercial assembly. We would like to thank Brian Carlisle and Randy Brost for suggesting such experiments, and Kevin Lynch for his elegant toppling analysis. We would also like to thank RP Berretty and Mark Overmars for their contributions to our thinking about the toppling graph.

References

[1] G. Causey and R. Quinn. Gripper Design Guidelines for Modular Manufacturing. In *IEEE International Conference on Robotics and Automation*, Leuven, Belgium, May 1998.

[2] J. Pertin-Troccaz. Grasping: A State of Art. In *The Robotics Review:1*. T. Lozano-Perez, Ed. MIT Press, 1989.

[3] X. Markenscoff, L. Ni and C. Papadimitriou. The Geometry of Grasping. *International Journal of Robotics Research*, Vol. 9, No. 1, February 1990.

[4] M. Mason and J. Salisbury. *Robotic Hands and the Mechanics of Manipulation*, MIT Press, 1985.

[5] J. Trinkle. On the Stability and Instantaneous Velocity of Grasped Frictionless Objects. *IEEE Transaction on Robotics and Automation*, Vol. 8, No. 5, October, 1992.

[6] J. Trinkle and R. Paul. Planning for Dexterous Manipulation with Sliding Contacts. *International Journal of Robotics Research*, Vol. 9, No. 3, June 1990.

[6] R. Brost. Automatic Grasping Planning in the Presence of Uncertainty. *International Journal on Robotics and Automation*, Vol. 7, No. 1, February, 1988.

[7] M. Peshkin and A. Sanderson. The Motion of a Pushed, Sliding Workpiece. *IEEE Transaction on Robotics and Automation*, Vol. 4, No. 6, 1989.

[8] D. Rus. Deterous Rotations of Polyhedra. In *IEEE International Conference on Robotics and Automation*, Nice, France, May, 1992.

[9] J. Hong, G. Lafferriere, B. Mishra and X, Tan. Fine Manipulation with Multifinger hands. In *IEEE International Conference on Robotics and Automation*, Cincinnati, Ohio, May, 1990.

[10] R. Fearing. Simplified Grasping and Manipulation with Detrous Robot hands. *International Journal on Robotics and Automation*, Vol. RA-2, No. 4, December, 1986.

[11] A. Bicchi and R. Sorrentino. Dextrous Manipulation Through Rolling. In *IEEE International Conference on Robotics and Automation*, Nagoya, Japan, May, 1995.

[12] A. Rao, D. Kriegman and K. Goldberg. Complete Algorithm for Feeding Polyhedral Parts Using Pivot Grasps. *IEEE Transaction on Robotics and Automation*, Vol. 12, No. 2, April, 1996.

[13] K. Lynch. Toppling Manipulation. In *IEEE International Conference on Robotics and Automation*, Detroit, MI, May 1999.

[14] T. Zhang, G. Smith, R. Berretty, M. Overmars, and K. Goldberg. The Toppling Graph: Designing Pin Sequences for Part Feeding. In *IEEE International Conference on Robotics and Automation*, San Francisco, CA, April 2000 (submitted).

[15] K. Goldberg. Orienting polygonal parts without sensors. *Algorithmica*, 10(2):201-225, August, 1993. Special Issue on Computational Robotics.

[16] M. T. Mason. Two Graphical Methods for Planar Contact Problems. In *IEEE/RSJ International Workshop on Intelligent Robots and Systems*, Pages 443-448, Osaka, Japan, November, 1991.

[17] T. Zhang, G. Smith, and K. Goldberg. Compensatory Grasping with the Parallel Jaw Gripper. Technical Report, ALPHA lab, UC Berkeley, 1999.

[18] F. van der Stappen, C. Wentink and M. Overmas. Computing Form-Closure Configurations. In *IEEE International Conference on Robotics and Automation*, Detroit, MI, May, 1999.